UC San Diego

UC San Diego Previously Published Works

Title

An interleukin-17-mediated paracrine network promotes tumor resistance to anti-angiogenic therapy.

Permalink

https://escholarship.org/uc/item/68j0k9h0

Journal

Nature medicine, 19(9)

ISSN

1078-8956

Authors

Chung, Alicia S
Wu, Xiumin
Zhuang, Guanglei
et al.

Publication Date

2013-09-01

DOI

10.1038/nm.3291

Peer reviewed

eScholarship.org Powered by the California Digital Library
University of California

nature medicine

An interleukin-17–mediated paracrine network promotes tumor resistance to anti-angiogenic therapy

Alicia S Chung[1], Xiumin Wu[1], Guanglei Zhuang[1], Hai Ngu[2], Ian Kasman[3,7], Jianhuan Zhang[4], Jean-Michel Vernes[4], Zhaoshi Jiang[5], Y Gloria Meng[4], Franklin V Peale[2], Wenjun Ouyang[6] & Napoleone Ferrara[1,7]

Although angiogenesis inhibitors have provided substantial clinical benefit as cancer therapeutics, their use is limited by resistance to their therapeutic effects. While ample evidence indicates that such resistance can be influenced by the tumor microenvironment, the underlying mechanisms remain incompletely understood. Here, we have uncovered a paracrine signaling network between the adaptive and innate immune systems that is associated with resistance in multiple tumor models: lymphoma, lung and colon. Tumor-infiltrating T helper type 17 (T_H17) cells and interleukin-17 (IL-17) induced the expression of granulocyte colony-stimulating factor (G-CSF) through nuclear factor κB (NF-κB) and extracellular-related kinase (ERK) signaling, leading to immature myeloid-cell mobilization and recruitment into the tumor microenvironment. The occurrence of T_H17 cells and Bv8-positive granulocytes was also observed in clinical tumor specimens. Tumors resistant to treatment with antibodies to VEGF were rendered sensitive in IL-17 receptor (IL-17R)-knockout hosts deficient in T_H17 effector function. Furthermore, pharmacological blockade of T_H17 cell function sensitized resistant tumors to therapy with antibodies to VEGF. These findings indicate that IL-17 promotes tumor resistance to VEGF inhibition, suggesting that immunomodulatory strategies could improve the efficacy of anti-angiogenic therapy.

© 2013 Nature America, Inc. All rights reserved.

The process of blood vessel formation is limited under steady-state conditions but becomes reactivated during a variety of pathological conditions, such as tumorigenesis. As angiogenesis is generally accepted to be a rate-limiting step during tumor growth, anti-angiogenic agents that target the VEGF–VEGF receptor signaling pathway have become an important component of therapy in multiple cancers[1]. However, similarly to other anticancer therapies, inherent and/or acquired resistance to anti-angiogenic drugs may occur in patients, leading to disease progression[2,3]. While there is need for improving the overall clinical efficacy and benefit of anti-angiogenic agents in treating cancer, the detailed mechanisms of resistance to treatment using antibodies to VEGF in patients with cancer remain to be determined.

Cancers develop in a complex host-tissue microenvironment comprised of immune cells, fibroblasts, blood and lymphatic vascular networks and the extracellular matrix[4]. In addition to host-mediated pathways[5], the crucial role of the microenvironment in tumor progression and response to therapy has become increasingly recognized[6,7]. However, an integrated understanding of drug resistance in the context of inputs from the tumor and the tumor microenvironment is lacking. Such mechanistic insights could be crucial for designing more effective therapies to overcome resistance to anti-angiogenic therapies.

Cancerous cells establish the tumor microenvironment through co-option of non-neoplastic stroma[6]. Whereas tumor cell–intrinsic drug resistance that is acquired after treatment typically develops gradually over time, tumor stroma–mediated drug resistance can occur rapidly due to changes in signaling events within the tumor microenvironment and theoretically can be reversed by removal or blockade of the tumor-stroma interaction.

This hypothesis prompted us to investigate tumor-stroma interactions that are important in mediating resistance to VEGF inhibition. We uncovered a paracrine network with the cytokine IL-17 at its core that mediates tumor resistance to VEGF blockade. IL-17 is the major effector cytokine of T_H17 cells, a subtype of adaptive immunity cells. These cells have an active role in inflammation and autoimmune diseases and have received much interest recently as modulators of tumor progression[8,9] However, how T_H17 cells affect tumor progression or antitumor immunity seems to depend on cancer type (reviewed in ref. 10). Here we have studied the role of T_H17 cells and IL-17 signaling in modulating the response to therapeutic VEGF inhibition in several syngeneic tumor models.

RESULTS

IL-17 is associated with refractory tumors

Recent evidence has demonstrated the role of the tumor microenvironment in mediating drug resistance (reviewed in refs. 6,7). An important question arising from this work is how tumor 'education' of normal stroma leads to drug resistance, particularly resistance

[1]Department of Research Drug Discovery, Genentech, Inc., South San Francisco, California, USA. [2]Department of Research Pathology, Genentech, Inc., South San Francisco, California, USA. [3]Department of Molecular Biology, Genentech, Inc., South San Francisco, California, USA. [4]Biocellular and Cellular Pharmacology, Genentech, Inc., South San Francisco, California, USA. [5]Department of Bioinformatics and Computational Biology, Genentech, Inc., South San Francisco, California, USA. [6]Department of Immunology, Genentech, Inc., South San Francisco, California, USA. [7]Present addresses: Department of Pathology and Moores Cancer Center, University of California San Diego, La Jolla, California, USA (N.F.) and Tinsley Research, LLC, Piedmont, California, USA (I.K.).

Received 5 March; accepted 1 July; published online 4 August 2013; doi:10.1038/nm.3291

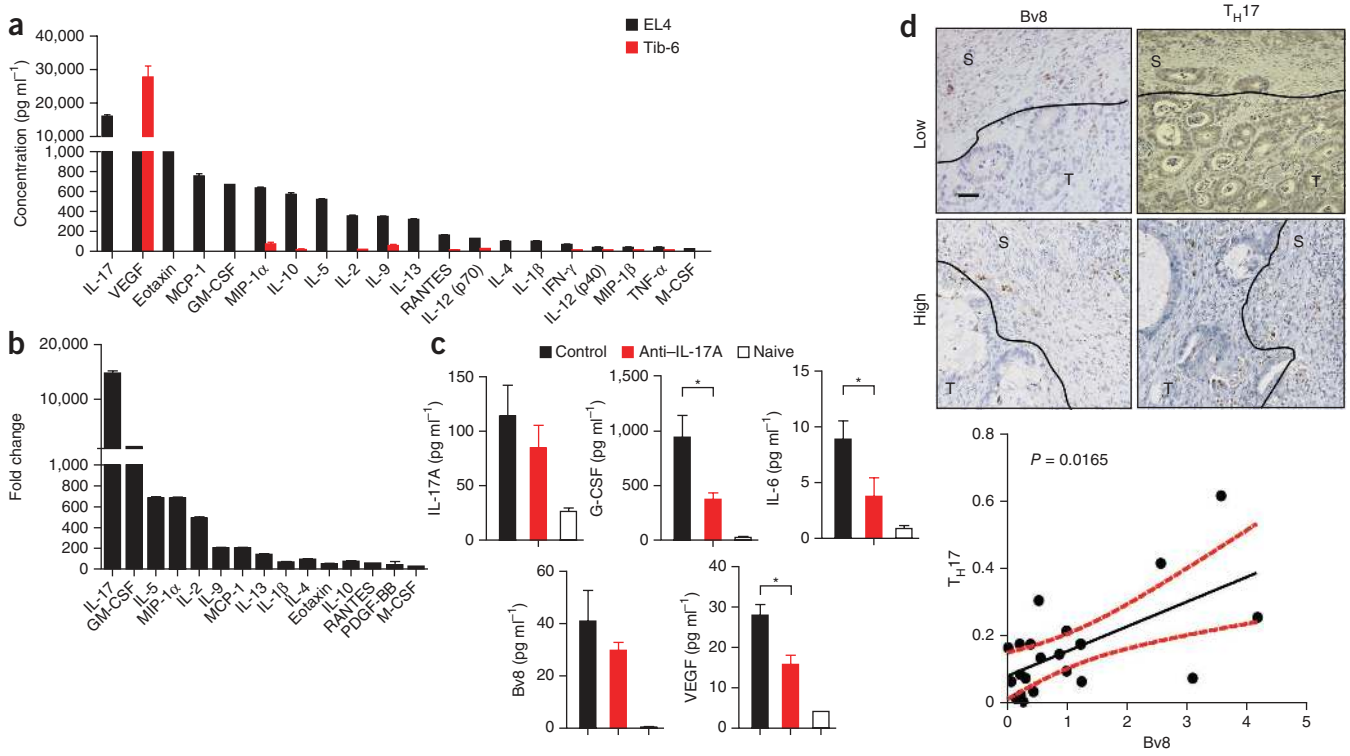

Figure 1 The role of soluble factors in mediating resistance to antibodies to VEGF and identification of IL-17 as the most abundant cytokine in a refractory tumor type. (**a**) Comparison of factors in the conditioned medium of tumor cell lines resistant (EL4) or sensitive (Tib-6) to antibodies to VEGF. (**b**) The ratios of soluble factors found in EL4 compared to Tib-6 cells sorted from highest to lowest amounts. (**c**) Changes in the amounts of secreted cytokines when IL-17A is neutralized *in vivo*. Shown are serum concentrations of G-CSF, IL-6, VEGF, Bv8 and IL-17 in EL4 tumor–bearing mice after treatment with an antibody to IL-17 or an isotype control antibody to ragweed (both at 10 mg per kg body weight) compared to tumor-naive mice ($n = 5$ per group). The data are shown as the mean ± s.e.m. $^*P < 0.05$ by Student's t test. (**d**) Top, representative images of colorectal tumors stained for Bv8 or IL-17A (T_H17 cells) expressing high or low amounts of Bv8 compared to IL-17A. S, stroma; T, tumor. Lines indicate the tumor-stroma boundary. Scale bar, 50 μm. Bottom, correlation of IL-17A–positive lymphocytes and Bv8-expressing granulocytes in a colorectal cancer cohort as determined by relative immunohistochemistry staining intensity (bottom, the best-fit line is indicated together with 95% confidence bands). Each dot represents an individual tumor sample. Spearman correlation 95% confidence interval, 0.09262–0.7695.

© 2013 Nature America, Inc. All rights reserved.

npg

to therapy using antibodies to VEGF. We hypothesized that tumors achieve this resistance through secreted factors. We addressed this issue by profiling tumor cell-secreted proteins using our well-characterized tumor models that are resistant (EL4) or sensitive (Tib-6) to treatment with antibodies to VEGF[11–13]. Our analysis revealed that the most abundantly secreted protein in the conditioned medium of EL4 cells, as well as the most differentially expressed cytokine compared to the sensitive cell line, was IL-17A, the canonical cytokine of the T_H17 subset of T cells (hereafter referred to as IL-17) (**Fig. 1a**,**b**).

Prompted by these findings, we investigated the role of IL-17 in the modulation of the tumor response to treatment with antibodies to VEGF. IL-17, also known as CTLA8, is a proinflammatory cytokine that has been implicated in autoimmunity, inflammation and cancer[14]. To determine whether IL-17 affects the tumor-associated stromal-cell phenotype, we performed an *in vivo* screen of circulating secreted factors in tumor-bearing mice, as assessment of the multiple potential target cell types for IL-17 needs to be done in an intact animal[15]. As the *in vitro* results for IL-17 production by EL4 cells were recapitulated *in vivo* in tumor-bearing animals (**Fig. 1c**), we next examined the amounts of proinflammatory factors known to be induced by IL-17. We found that the amounts of G-CSF and IL-6 were similarly increased in tumor-bearing mice (**Fig. 1c**), whereas the amounts of other IL-17–inducible factors, such as chemokine (C-X-C motif) ligand 1 (CXCL1), CXCL2, tumor necrosis factor-α (TNF-α) and IL-1β, were unchanged compared to tumor-naive mice (data not shown). Notably, EL4 tumor–bearing mice also had an increased amount of prokineticin 2 (Bv8, also called PROK2) (**Fig. 1c**), a G-CSF–inducible angiogenic factor[16] that has been previously reported to mediate tumor refractoriness to VEGF blockade[17]. Administration of a neutralizing antibody to IL-17A *in vivo* significantly reduced the amounts of G-CSF, IL-6 and VEGF and lowered the amount of Bv8 in the circulation of tumor-bearing mice (**Fig. 1c**). That treatment with the IL-17–specific antibody did not markedly change the amount of IL-17 (**Fig. 1c**) probably reflects the inability of the assay to distinguish free from antibody-bound IL-17. Addition of this antibody to IL-17 inhibited ~70% of EL4 cell–induced G-CSF secretion by fibroblasts in coculture (**Supplementary Fig. 1c**), confirming its neutralizing activity against IL-17. In contrast, antibody neutralization of other known G-CSF inducers, including TNF-α and IL-1β, both of which are secreted by the refractory tumor, had little or no effect on the circulating concentration of G-CSF (**Supplementary Fig. 1c**). Together these data suggest that IL-17 has a dominant role in regulating the systemic amounts of soluble factors involved in inflammation and angiogenesis.

We next looked for evidence of IL-17 involvement in 23 advanced-stage human colorectal adenocarcinoma specimens. We found that the number of IL-17 immunopositive tumor-infiltrating T_H17

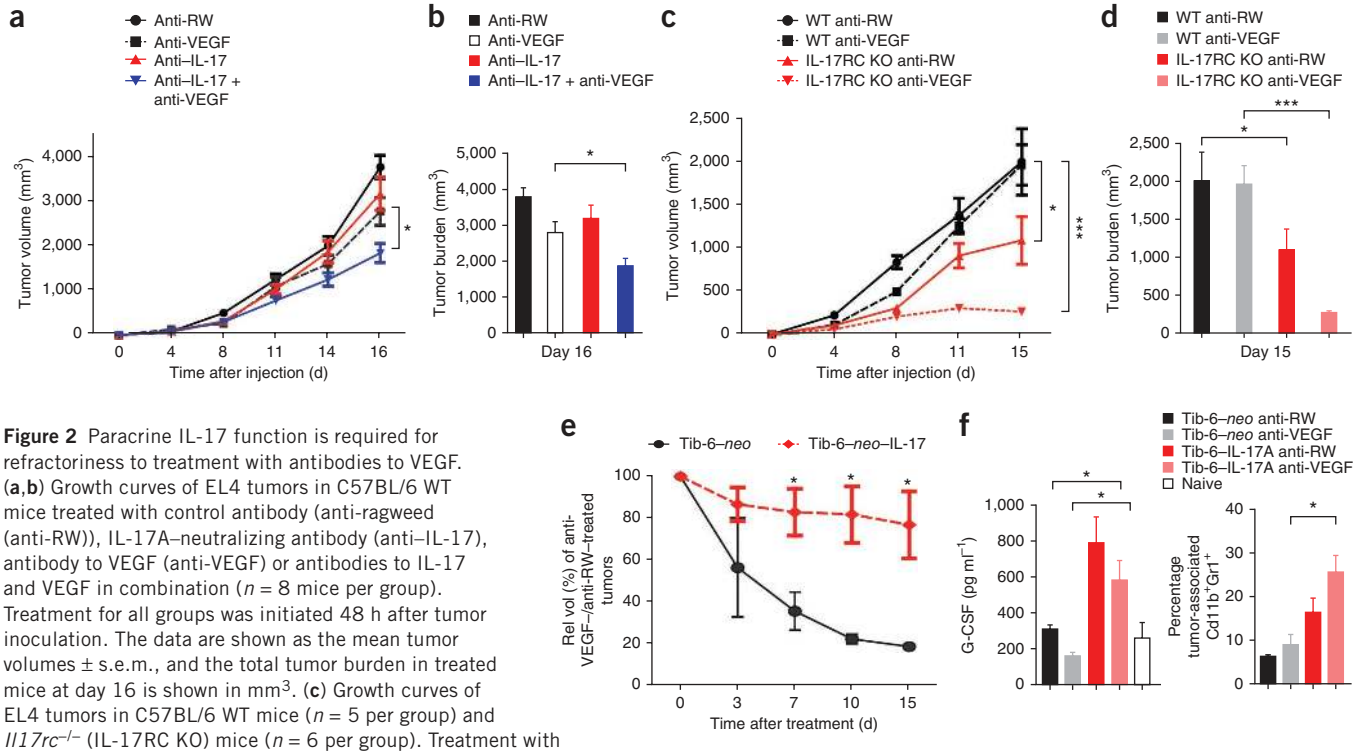

Figure 2 Paracrine IL-17 function is required for refractoriness to treatment with antibodies to VEGF. (**a**,**b**) Growth curves of EL4 tumors in C57BL/6 WT mice treated with control antibody (anti-ragweed (anti-RW)), IL-17A–neutralizing antibody (anti–IL-17), antibody to VEGF (anti-VEGF) or antibodies to IL-17 and VEGF in combination ($n = 8$ mice per group). Treatment for all groups was initiated 48 h after tumor inoculation. The data are shown as the mean tumor volumes ± s.e.m., and the total tumor burden in treated mice at day 16 is shown in mm^3. (**c**) Growth curves of EL4 tumors in C57BL/6 WT mice ($n = 5$ per group) and *Il17rc*$^{-/-}$ (IL-17RC KO) mice ($n = 6$ per group). Treatment with antibodies to VEGF or control antibodies to ragweed was initiated 48 h after tumor inoculation. The data are shown as the mean tumor volumes ± s.e.m. (**d**) Total tumor burden in WT and *Il17rc*$^{-/-}$ mice treated with antibodies to ragweed or VEGF at day 15 (shown in mm^3) ($n = 5$–6 per group). (**e**) Relative tumor volume of Tib-6–neo tumor cells (control) and Tib-6 tumor cells stably expressing IL-17A (Tib-6–IL-17) treated with antibodies to VEGF or ragweed. Results are representative of independent experiments with two Tib-6–neo control and four Tib-6–IL-17 cell lines. $n = 8$ mice per treatment group. Rel vol, relative volume. (**f**) Serum G-CSF concentrations and the number of tumor-infiltrating $CD11b^+Gr1^+$ cells in Tib-6–neo and Tib-6–IL-17 tumors ($n = 5$–8 per group). The data (**d**–**f**) are shown as the mean ± s.e.m. $^*P < 0.05$, $^{***}P < 0.0005$ by Student's *t* test.

lymphocytes correlated significantly with the number of tumor-associated Bv8-expressing neutrophils, particularly surrounding the tumor margins (**Fig. 1d** and **Supplementary Fig. 1a**,**b**). This result suggests a functional link between these two cell types, whose influx into tumors is associated with poor outcome in colorectal cancer as well as in hepatocellular and lung carcinomas[10].

Refractoriness to VEGF-specific antibodies requires IL-17

To further investigate the role of IL-17 in the tumor microenvironment *in vivo*, we used three experimental systems (**Fig. 2**). First, we used the EL4 cell line in a syngeneic transplant system. This cell line is resistant to treatment with antibodies to VEGF and, similarly to T_H17 cells, expresses both IL-17A and the closely related cytokine IL-17F (**Supplementary Fig. 1d**). We treated EL4 tumor-bearing mice with antibodies to VEGF alone and in combination with an IL-17A–neutralizing antibody. Second, we implanted EL4 cells into C57BL/6 (wild type, WT) and IL-17R–deficient mice (*Il17rc*$^{-/-}$, hereafter referred to as knockout mice). IL-17RA and IL-17RC form a heterodimeric receptor complex that is required for IL-17 signaling in humans and mice, and knockout mice are nonresponsive to IL-17 signaling inputs18. Third, we used an allograft model in which we tested the effects of IL-17A expression in tumor cells (Tib-6) that are sensitive to treatment with antibodies to VEGF.

Treatment of EL4 tumor–bearing mice with a monoclonal antibody to IL-17A in combination with antibodies to VEGF improved the response to the VEGF-specific antibodies and inhibited tumor growth by ~50% compared to mice treated with an antibody specific for an irrelevant protein, ragweed, a control. Inhibition of IL-17A signaling without VEGF antibody treatment had only a slight effect on tumor growth (**Fig. 2a**,**b**). In the second experimental system, we tested the growth and drug response of EL4 tumors in WT mice compared to knockout littermates (**Fig. 2c**,**d**). In the control treatment groups without VEGF antibody treatment, EL4 tumor volume was reduced by ~50% in knockout mice compared to WT mice, suggesting that IL-17 signaling in the host stroma has a role in tumor growth, a result which is potentially related to our finding that VEGF expression in EL4-tumor bearing mice is IL-17 dependent (**Fig. 1c**). Notably, IL-17R deficiency resulted in an almost 80% tumor growth inhibition by treatment with antibodies to VEGF compared to the modest effects such antibodies had in WT mice. The loss of IL-17 signaling in host stromal cells had a more marked effect on tumor growth in this genetic mouse model compared to pharmacologic neutralization of IL-17A, potentially because of insufficient *in vivo* neutralization of heterodimeric IL-17A and IL-17F and homodimeric IL-17F species by antibodies to IL-17A. To address this possibility, we tested an IL-17F–neutralizing antibody, both alone and in combination with antibodies to IL-17A, in EL4 tumor–bearing mice. The combination of the two types of antibodies did not offer further attenuation of tumor growth compared to antibodies to IL-17A only (**Supplementary Fig. 1d**,**e**), suggesting that IL-17F has little effect on tumor growth. Therefore, the greater inhibition of tumor growth in the genetic model likely reflects a more complete or persistent inhibition of IL-17R signaling than that achieved through pharmacological means. Taken together these data suggest that tumor growth and the antitumor effects of VEGF blockade are dependent on IL-17 signaling within the host tumor microenvironment. Notably, these effects are dependent on

© 2013 Nature America, Inc. All rights reserved.

modulation of the host response by IL-17 but not on IL-17 autocrine function in tumor cells, as EL4 tumor cells lack IL-17R expression (**Supplementary Fig. 1f**).

We confirmed that our refractory model was truly VEGF independent in dose-response studies using VEGF-specific antibodies that showed saturation of antitumor efficacy with the lowest dose of antibody tested (5 mg per kg body weight) and by ELISA assays demonstrating that the amounts of VEGF-specific antibody were in excess of those of its target ligand within the tumor (**Supplementary Fig. 2a**,**b**). It is also unlikely that IL-17 directly induces VEGF systemically, as naive mice treated with an IL-17A–specific antibody did not have markedly altered amounts of VEGF and VEGF amounts did not differ significantly between EL4 tumor–bearing WT and knockout mice (**Supplementary Fig. 2c**,**d**). However, a direct role of IL-17 in facilitating tumor angiogenesis was suggested by *in vitro* assays (**Supplementary Fig. 2e**), further implicating a direct angiogenic function for IL-17.

To further test the role of IL-17 in mediating tumor resistance to VEGF inhibition, we transduced a treatment-sensitive tumor cell line, Tib-6, with mouse IL-17A (generating Tib-6–IL-17 cells) or with neomycin (generating Tib-6–neo cells) and tested the response of the transduced cells to treatment with antibodies to VEGF when implanted into immunodeficient (*nu*/*nu*) recipient mice. Tib-6–IL-17-tumor bearing mice had markedly higher amounts of both circulating and tumor-localized IL-17A compared to Tib-6–neo-tumor bearing mice (data not shown). We also detected higher amounts of G-CSF in Tib-6–IL-17 tumors than in Tib-6–neo-tumors, and Tib-6–IL-17 tumors recruited more $CD11b^+Gr1^+$ cells than did Tib-6–neo tumors (**Fig. 2f**). Although Tib-6–IL-17 tumors did not show a substantial increase in tumor growth rate compared to Tib-6–neo tumors (**Supplementary Fig. 1g**), they were significantly more resistant to treatment with antibodies to VEGF, as assessed using four independent stable Tib-6–IL-17 cell lines compared to two Tib-6–neo control cell lines (**Fig. 2e**). These gain-of-function data in *nu/nu* mice indicate that IL-17 effector function can occur independently of additional inputs from T cells, suggesting that IL-17 function is both necessary and sufficient to mediate a proinflammatory network that drives therapeutic resistance to antibodies to VEGF.

IL-17 mediates $CD11b^+Gr1^+$ cell mobilization and recruitment

To investigate the role of IL-17 signaling in the tumor microenvironment, we sought to better characterize differences in the tumor milieu in WT compared to $Il17rc^{-/-}$ hosts. Serum concentrations of IL-17A were similarly elevated in WT and knockout mice bearing EL4 tumors compared to tumor-naive mice (**Fig. 3a**,**b**). We screened known IL-17A–inducible proinflammatory factors and found significant increases in the amounts of only G-CSF and IL-6 in WT tumor-bearing compared to naïve mice (**Fig. 3a**). In contrast, the serum concentration of G-CSF was not elevated in KO tumor-bearing compared to naïve mice (**Fig. 3b**), providing further evidence that IL-17 signaling to the host stroma is required for G-CSF induction *in vivo*. Treatment with antibodies to VEGF did not change the serum concentrations of IL-17A, G-CSF or IL-6 in tumor-bearing WT or KO mice (**Fig. 3b**). On the basis of these results, we postulate that IL-17 mediates systemic inflammation through paracrine mechanisms. Notably, the serum concentrations of monocyte chemoattractants, including CCL2, CCL3, CCL4 and CCL5, remained relatively unchanged between WT and knockout tumor-bearing mice (**Supplementary Fig. 3a**). Likewise, the amounts of these factors were not induced in the IL-17 gain-of-function tumor model (**Supplementary Fig. 3b**). These results suggest that IL-17 does not elicit a specific monocytic proinflammatory program within the tumor microenvironment and that monocytes may not be the primary drivers of treatment refractoriness to VEGF-specific antibodies.

G-CSF is a principal regulator of granulopoiesis and has a key role in neutrophil mobilization from the bone marrow in response to a variety of environmental stresses[19,20]. It is also known to mobilize immature myeloid cells, including precursors of granulocytes, macrophages and dendritic cells, that express both CD11b and Gr1. Despite this cell type and functional heterogeneity, this cell population is frequently referred to collectively as myeloid-derived suppressor cells (MDSCs). Consistent with effects on G-CSF serum concentrations, circulating concentrations of $CD11b^+Gr1^+$ cells were likewise elevated threefold in WT tumor-bearing mice compared to knockout tumor-bearing hosts and tumor-naive mice (**Fig. 3c**,**d**). Furthermore, the numbers of tumor-infiltrating $CD11b^+Gr1^+$ cells were significantly lower in knockout compared to WT hosts, as assesed by flow cytometry and immunofluorescent staining of tumor sections (**Fig. 3d**,**e**). There were no statistically significant differences in the number of $F4/80^+$ tumor-associated macrophages (**Supplementary Fig. 3c**).

Within tumors of WT mice, we found that the $CD11b^+Gr1^+$ population represented a granulocytic $CD11b^+Gr1^{hi}$ MDSC population that was negative for the $F4/80^+$ macrophage marker, whereas a cell population with intermediate $Gr1^+$ staining intensity was characterized by $F4/80^{-/lo}$ expression, and $CD11b^+Gr1^{lo/-}$ cells were predominantly $F4/80^+$ macrophages (**Supplementary Fig. 4a**). The $CD11b^+Gr1^{hi}$ population in the spleen and bone marrow was reduced in tumor-bearing knockout compared to WT mice (**Supplementary Fig. 4c**,**d**), suggesting a role for IL-17 paracrine signaling in the maintenance and development of these immune-suppressive cells.

To test the requirement for G-CSF in mediating treatment refractoriness to antibodies to VEGF, we implanted the resistant EL4 cell line into syngeneic G-CSF receptor (G-CSFR) knockout mice ($Csf3r^{-/-}$, hereafter referred to as G-CSFR knockout mice), in which all stromal host cells are deficient in G-CSF signaling. We observed that although G-CSF signaling did not seem to have a major impact on the growth of EL4 tumors, this signaling axis was indeed necessary in mediating tumor refractoriness to treatment with antibodies to VEGF, and was also necessary for $CD11b^+Gr1^+$ cell mobilization from the bone marrow and recruitment to the tumor microenvironment (**Fig. 3f**). Together these data demonstrate the requirement for an IL-17–G-CSF signaling cascade in mediating resistance to antibodies to VEGF through the mobilization and recruitment of $CD11b^+Gr1^+$ cells to the tumor microenvironment.

IL-17 regulates immature myeloid cell effector function

Because $CD11b^+Gr1^+$ immature myeloid cells are known to drive tumor progression through immunosuppression and tumor angiogenesis (reviewed in refs. 21,22), we tested whether loss of IL-17 signaling affected these effector functions. To address this question, we first tested the ability of these cells to suppress T cell proliferation. The immunosuppressive function of $CD11b^+Gr1^+$ cells isolated from WT tumors was readily apparent but was missing from the same cells isolated from knockout hosts (**Fig. 4a**). To get a more complete picture of IL-17–dependent effector functions, we performed gene expression profiling of $CD11b^+Gr1^+$ cells isolated from tumors of WT and knockout littermates. We found that loss of IL-17 signaling correlated with decreased expression of effector genes, including those encoding the proangiogenic factor Bv8, metalloprotease-9 (MMP-9) and the inflammation and cancer-promoting factors S100A8 and S100A9

© 2013 Nature America, Inc. All rights reserved.

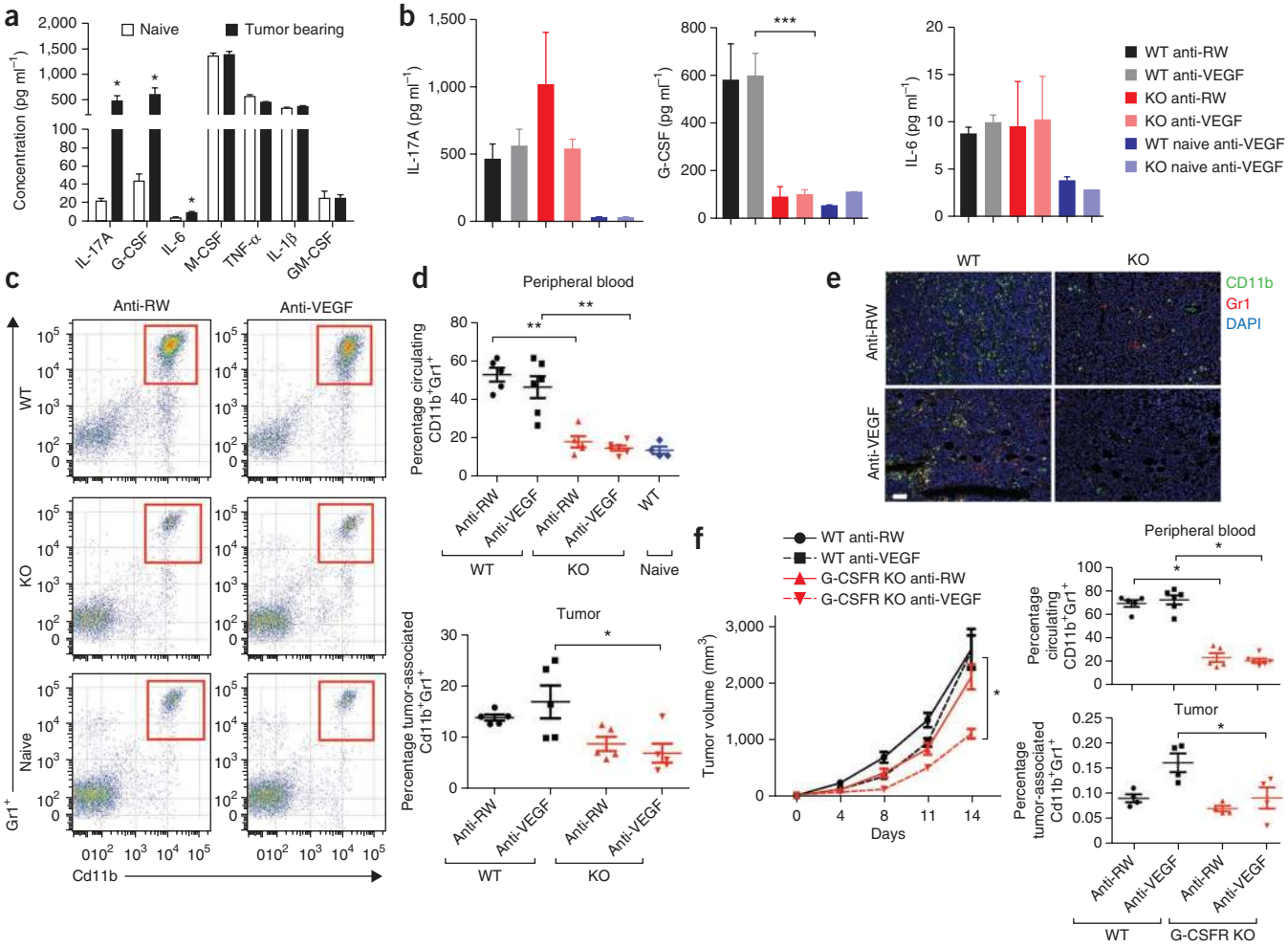

Figure 3 IL-17 signaling is required for the mobilization and tumor infiltration of CD11b$^+$Gr1$^+$ cells. (**a**) Amounts of proinflammatory cytokines in the serum of EL4 tumor–bearing mice compared to tumor-naive littermates ($n = 6$ per group). (**b**) Serum IL-17, G-CSF and IL-6 concentrations in EL4 tumor–bearing WT and *Il17rc*$^{-/-}$ (KO) mice in response to control treatment (antibodies to ragweed) or treatment with antibodies to VEGF ($n = 6$ per group). (**c**) Numbers of CD11b$^+$Gr1$^+$ cells (gated in red boxes) in circulation in tumor-bearing WT and *Il17rc*$^{-/-}$ hosts as determined by flow cytometric analysis. (**d**) Quantification of flow cytometric analyses of circulating (top) and tumor-infiltrating (bottom) CD11b$^+$Gr1$^+$ cells ($n = 5$–6 per group). (**e**) Representative immunofluorescence images of tumor-infiltrating CD11b$^+$Gr1$^+$ cells. Shown is CD11b (green) and Gr1 (red) staining of EL4 tumors from WT and *Il17rc*$^{-/-}$ mice treated with the control antibody to ragweed or antibodies to VEGF. Scale bar, 10 μm. (**f**) Left, growth curves of EL4 tumors in C57BL/6 WT mice and G-CSFR knockout mice ($n = 5$ mice per group). Treatment with antibodies to VEGF or control antibodies to ragweed was initiated 48 h after tumor inoculation. Right, quantification of the number of CD11b$^+$Gr1$^+$ cells entering the circulation (top) and those infiltrating the tumor (bottom) in tumor-bearing WT compared to G-CSFR knockout hosts as determined by flow cytometric analysis. All data are shown as the mean ± s.e.m. $^*P < 0.05$, $^{**}P < 0.005$, $^{***}P < 0.0005$ by Student's *t* test.

(low–molecular weight calcium-binding proteins that have been implicated in MDSC recruitment and enhancement of MDSC activity[23]) (**Fig. 4b**). Using quantitative RT-PCR (qRT-PCR), we confirmed that expression of these effector genes was dependent on IL-17 signaling but was not affected by treatment with antibodies to VEGF (**Fig. 4b**), suggesting a role for IL-17 signaling in the regulation of CD11b$^+$Gr1$^+$ effector function.

To further delineate the functional contribution of CD11b$^+$Gr1^{hi}F4/80$^-$ granulocytic MDSCs and CD11b$^+$Gr1$^{lo/-}$F4/80$^+$ tumor–associated macrophages (TAMs) in the tumor microenvironment, we performed whole-genome expression analysis of these myeloid subpopulations in WT and *Il17rc* knockout tumor-bearing hosts (**Supplementary Fig. 4b**). Mannose receptor C type 1 (MRC1), a monocytic marker, has been previously shown to be enriched in the CD11b$^+$Gr1$^{lo/-}$F4/80$^+$ TAM population[24], and we confirmed this finding. Among other genes that have been reported to have immune-suppressive functions, the expression of inducible nitric oxide synthase (iNOS, also known as NOS2) was higher in granulocytic MDSCs and was dependent on intact IL-17 signaling in the tumor microenvironment, whereas arginase was more highly expressed in the CD11b$^+$Gr1$^{lo/-}$F4/80$^+$ TAM subset. Furthermore, we found expression of TGF-β1, IL-10, GAL9 (also known as LGALS9) and ADAM17, which have all been reported to effectuate MDSC immune-suppressive functions, to be more prevalent in the TAM subset (**Supplementary Fig. 4b**). Therefore, loss of IL-17 signaling results in attenuation of CD11b$^+$Gr1$^+$ cell recruitment as well as of the T cell–inhibition function of CD11b$^+$Gr1$^+$ cells and effector gene expression in these cells, allowing for the restoration of tumor sensitivity to VEGF blockade.

We further investigated the effects of IL-17 signaling on the tumor vasculature, as assessed by immunohistochemical detection of a

© 2013 Nature America, Inc. All rights reserved.

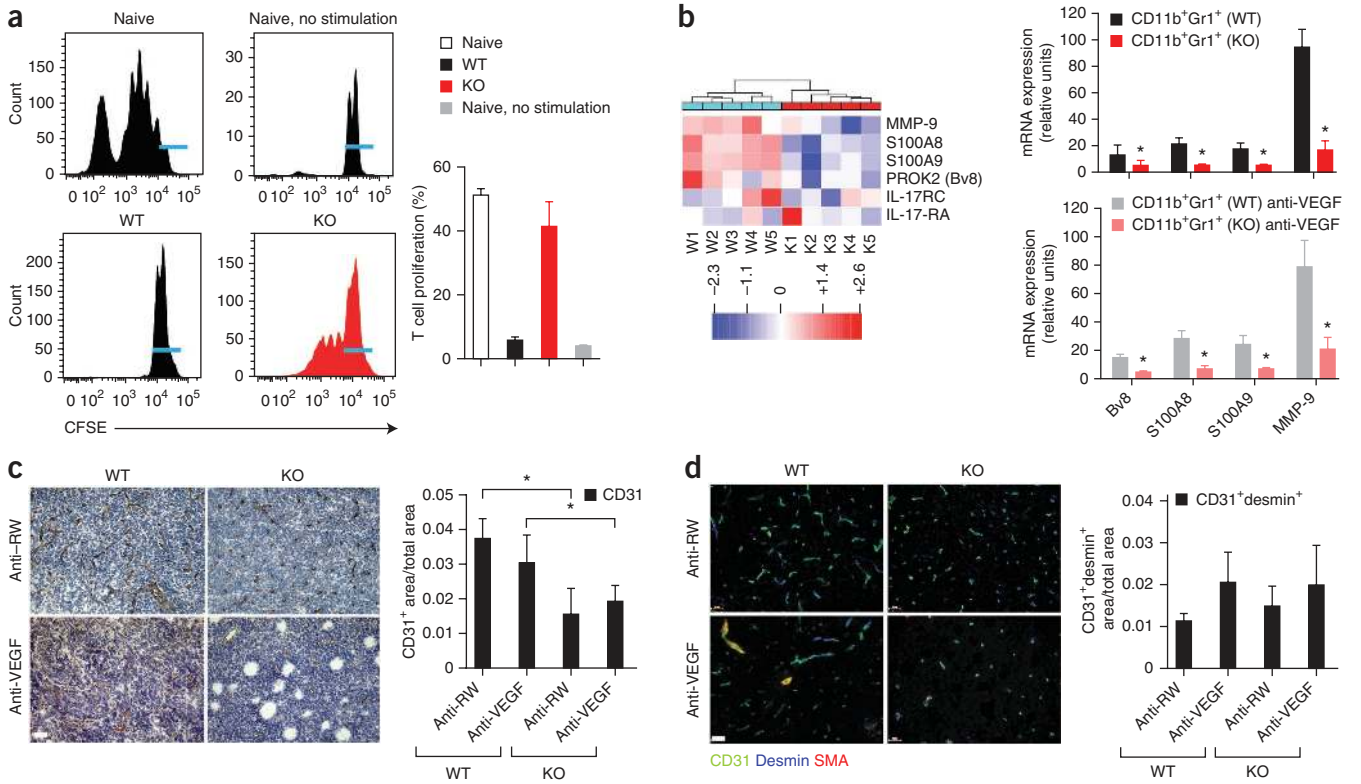

Figure 4 IL-17 signaling regulates the function of immature myeloid CD11b$^+$Gr1$^+$ cells from tumor-bearing mice and promotes tumor angiogenesis. (**a**) Effects of CD11b$^+$Gr1$^+$ cells isolated from EL4 tumor–bearing mice WT ($n = 6$) or *Il17rc*$^{-/-}$ mice ($n = 5$) on T cell proliferation. CD45$^+$CD11b$^+$Gr1$^+$ cells were isolated from tumors by magnetic separation and cocultured with naive CD4$^+$ T cells isolated from WT mouse spleens. Dilution of carboxyfluorescein succinimidyl ester (CFSE) staining in splenic T cells is shown on day 3 after T cell activation with antibodies specific to CD3 and CD28. Blue horizontal bars indicate the undiluted CFSE intensity on day 3. The data are representative of two independent experiments using CD11b$^+$Gr1$^+$ cells isolated from individual tumor-bearing or naive mice. As controls, T cells were either cocultured with CD11b$^+$Gr1$^+$ cells isolated from spleens of WT tumor-naive mice ($n = 4$; naive) or were left unstimulated (naive, no stimulation). (**b**) Microarray gene-expression (left) and qRT-PCR (right) analyses of CD45$^+$CD11b$^+$Gr1^{hi} cells isolated by magnetic separation from tumors of WT (W1–W5) and *Il17rc*$^{-/-}$ (K1–K5) mice. Representative qRT-PCR assays from two independent cohorts run in triplicate are shown, and the data are shown as the mean ± s.e.m. $^*P < 0.05$ by Student's *t* test. (**c**) Left, representative immunohistochemical images of the EL4 tumor vasculature in WT and knockout hosts treated with either control antibodies or antibodies to VEGF and stained for MECA-32 (brown) and counterstained with hematoxylin (blue). Right, quantification of the MECA-32–positive area compared to the total tumor area ($n = 5$ per group). Scale bar, 10 μm. (**d**) Left, representative immunofluorescence images of the tumor vasculature stained with CD31 (green) and smooth muscle actin (SMA, red) and of vasculature-associated pericytes stained with desmin (blue), revealing the vessel maturity of EL4 tumors in WT and knockout hosts after treatment with antibodies to VEGF. Right, quantification of the area of mature vessels per total tumor area ($n = 5$ per group). The data are shown as the mean ± s.e.m. Scale bar, 10 μm.

pan-endothelial marker antigen, MECA-32 (mouse endothelial cell antigen, clone 32); we also evaluated vessel maturation by immunofluorescent costaining for the endothelial cell adhesion junction protein PECAM-1 (also known as CD31) and desmin, a marker for pericytes (a vasculature-support cell type). Mean vessel density, quantified as immunopositivity for MECA-32, was significantly lower in tumors established in knockout as compared to WT hosts either with or without VEGF-specific antibody treatment (**Fig. 4c**). Notably, the percentage of pericyte-associated mature tumor vessels was greater after treatment with antibodies to VEGF in both WT and knockout hosts, consistent with the notion that VEGF blockade is efficient at pruning immature vessels and that IL-17 signaling has no significant effect on this process (**Fig. 4d**). Together these data suggest a role for IL-17 in modulating the tumor vasculature by directing the effector function of CD11b$^+$Gr1$^+$ cells independently of VEGF.

Tumor-associated fibroblasts are activated by IL-17

Ex vivo profiling of secreted proteins from FACS-isolated GFP$^+$ EL4 tumor cells and host stromal cells revealed that the stromal compartment is the primary source of major proinflammatory cytokines (**Fig. 5a**). To identify the stromal cell type responsible for proinflammatory cytokine production, we used platelet-derived growth factor receptor-α (PDGFR-α) as a cell-surface marker for sorting tumor-associated fibroblasts (TAFs), as this protein was recently reported to be expressed by TAFs in a number of tumor models[25]. PDGFR-α–positive cells also expressed additional TAF markers, including vimentin and smooth muscle actin (SMA), as detected by immunofluorescence; these cells also expressed fibroblast growth factor receptor-1 (FGFR1) but did not express myeloid lineage markers, including CXCR4 and MRC1, confirming the purity the sorted TAF cells (**Supplementary Fig. 5a**,**b**). We next investigated the relative levels of cytokine and chemokine secretion by TAFs, tumor-associated CD11b$^+$Gr1$^+$ MDSCs and nongranulocytic CD11b$^+$Gr1$^-$ myeloid lineage cells. We found higher levels of cytokine secretion by TAFs as compared to the other tumor-infiltrating myeloid cell types (**Fig. 5b**). Furthermore, cytokine analysis of freshly isolated TAFs from EL4 tumors in both WT and knockout recipients revealed reduced expression of G-CSF, IL-6 and granulocyte macrophage colony-stimulating factor (GM-CSF) in knockout TAFs,

© 2013 Nature America, Inc. All rights reserved.

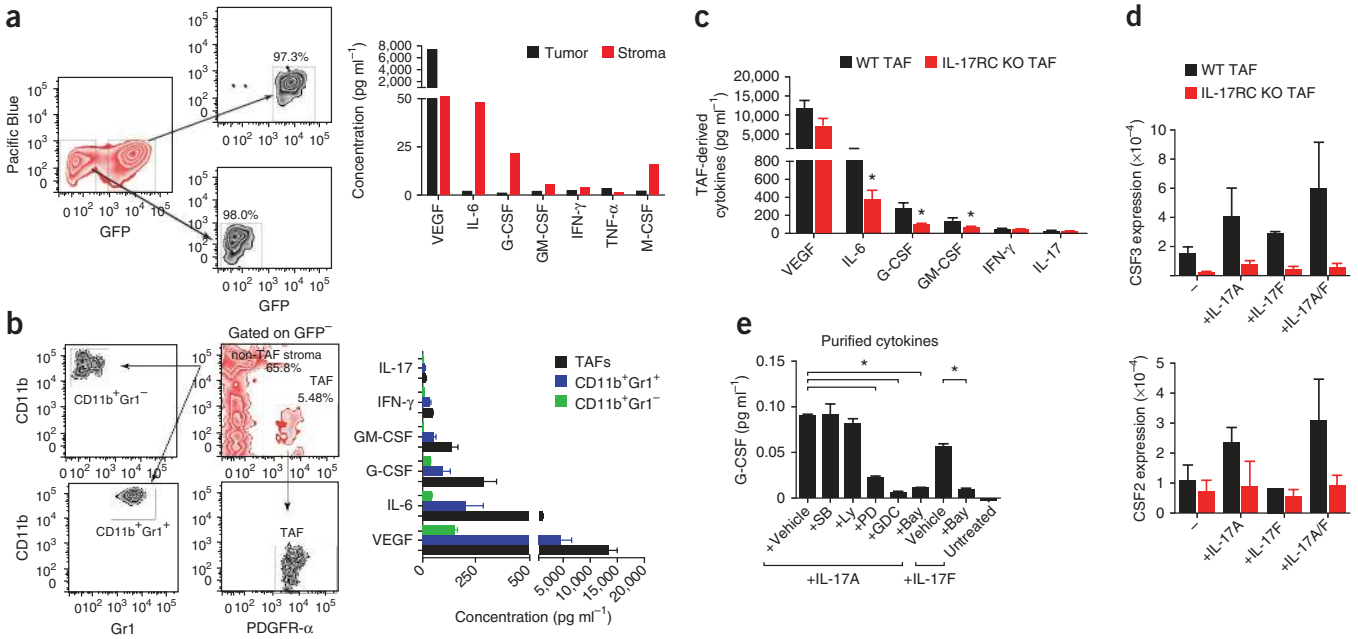

Figure 5 IL-17 induction of proinflammatory cytokines in tumor-associated fibroblasts is dependent on the activity of NF-κB and MEK1/2. (**a**) Secreted cytokines (right) analyzed *ex vivo* from GFP$^+$ tumor cells and GFP$^-$ stromal cells isolated by flow cytometry as shown (left) from EL4 tumors in C57BL/6 mice ($n = 5$ per group). (**b**) Cytokine and growth-factor profiling (right) in the conditioned media of TAFs (PDGFR-α$^+$) and tumor-infiltrating CD11b$^+$Gr1$^+$ and CD11b$^+$Gr1$^-$ cells that were isolated by flow cytometry as shown (left) from EL4 tumors ($n = 5$ per group). (**c**) Cytokines in the conditioned media from PDGFR-α$^+$ TAFs from WT and IL-17RC knockout mice, as assessed by cytokine bead arrays. The cells were isolated by flow cytometry and cultured *in vitro* for 72 h. (**d**) qRT-PCR analysis of CSF3 (G-CSF) and CSF2 (GM-CSF) in TAFs isolated from EL4 tumors from WT and *Il17rc*$^{-/-}$ mice. The TAFs were treated with purified mouse IL-17A (100 ng ml^{-1}), IL-17F (200 ng ml^{-1}) or the two in combination (IL-17A/F). The experiment was performed with primary TAFs *in vitro*, and the data represent three biological replicates. (**e**) G-CSF concentrations measured by ELISA in the cell culture supernatant from immortalized mouse fibroblasts that had been pretreated with the indicated inhibitors (SB98059 (SB), LY294002 (Ly), PD98059 (PD), GDC-0973 (GDC) or Bay11-7082 (Bay), all of which were used at 10 μM except for Bay11-7082 and GDC-0973, which were used at 1 μM) or vehicle (DMSO) for 30 min followed by the addition of purified IL-17A (100 ng ml^{-1}) or IL-17F (200 ng ml^{-1}) for 4 h. Representative assays from two independent cohorts run in triplicates are shown, and the data are shown as the mean ± s.e.m. *$P < 0.05$ by Student's *t* test.

whereas the expression of VEGF was not different (**Fig. 5c**); in fact, VEGF expression was not affected by IL-17 signaling in any of the stromal cell types studied (**Supplementary Fig. 3d**). Together these data support the notion that IL-17 signaling in TAFs controls a network of proinflammatory cytokines in the tumor milieu.

The proinflammatory cytokines IL-17A and IL-17F have a high degree of sequence similarity and share many biological properties[14]. In an *ex vivo* setting, WT but not knockout TAFs could be further stimulated by IL-17A or IL-17F to express proinflammatory cytokines such as G-CSF and GM-CSF (**Fig. 5d**). We conclude that the paracrine signaling function of IL-17 is necessary and sufficient for promoting phenotypic changes in fibroblasts within the tumor microenvironment.

IL-17A–IL-17F activation of target cells requires activation of the intracellular NF-κB, mitogen-activated protein kinase (MAPK) and C/EBP (also called CEBPA) signaling pathways to induce the expression of soluble factors, including G-CSF[14]. We therefore investigated whether these and additional intracellular signaling pathways were activated in TAFs in response to IL-17. Using a panel of signaling-pathway inhibitors, we found that MEK (also called MAP2K1) and NF-κB signaling are required for IL-17–induced G-CSF expression, as indicated by a reduction of G-CSF expression in fibroblasts treated with either of two different MEK inhibitors (PD98059 and GDC-0973) or with an NF-κB pathway inhibitor (Bay11-7082) but not with inhibitors targeting the phosphatidylinositide 3-kinase (PI3K) or p38 MAPK pathways (**Fig. 5e**). Together these data indicate that IL-17 is capable of inducing proinflammatory cytokines such as G-CSF in TAFs through MAPK and NF-κB signaling.

T_H17 cells mediate the response to VEGF-specific antibodies

IL-17 is produced by the T_H17 subset of CD4$^+$ and CD8$^+$ T cells (Tc17 cells)[26–28]. Because the infiltration of T_H17 cells is associated with poor prognosis in human lung and colorectal cancers[29–31], we sought to test the effect of tumor-infiltrating T_H17 cells in response to treatment with antibodies to VEGF in syngeneic mouse lung and colon cancer models. We observed a significant decrease in tumor burden in Lewis lung carcinoma (LLC)-bearing *Il17rc*$^{-/-}$ compared to WT littermates after treatment with antibodies to VEGF (**Fig. 6a**). In a lung orthotopic model in WT mice, we observed that treatment with a combination of VEGF-specific and IL-17AF-specific antibodies significantly reduced LLC^{luc+} (luciferase-expressing LLC) tumor burden compared to treatment with a VEGF-specific antibody alone ($P < 0.05$) (**Supplementary Fig. 5c,d**). Likewise, growth of a colorectal tumor, CT-26, was significantly reduced in syngeneic mice when treated with antibodies to IL-17 and VEGF in combination as compared to treatment with antibodies to VEGF alone (**Fig. 6a**).

We initially observed that the percentage of LLC tumor–infiltrating CD3$^+$ T cells did not differ between WT and knockout hosts (1.24% ± 0.18% (mean ± s.e.m.) and 1.28% ± 0.22% of live tumor cells, respectively). However, consistent with recent reports indicating that anti-angiogenic therapies can increase tumor lymphocyte infiltration[32–34], we found that treatment with antibodies to VEGF

© 2013 Nature America, Inc. All rights reserved.

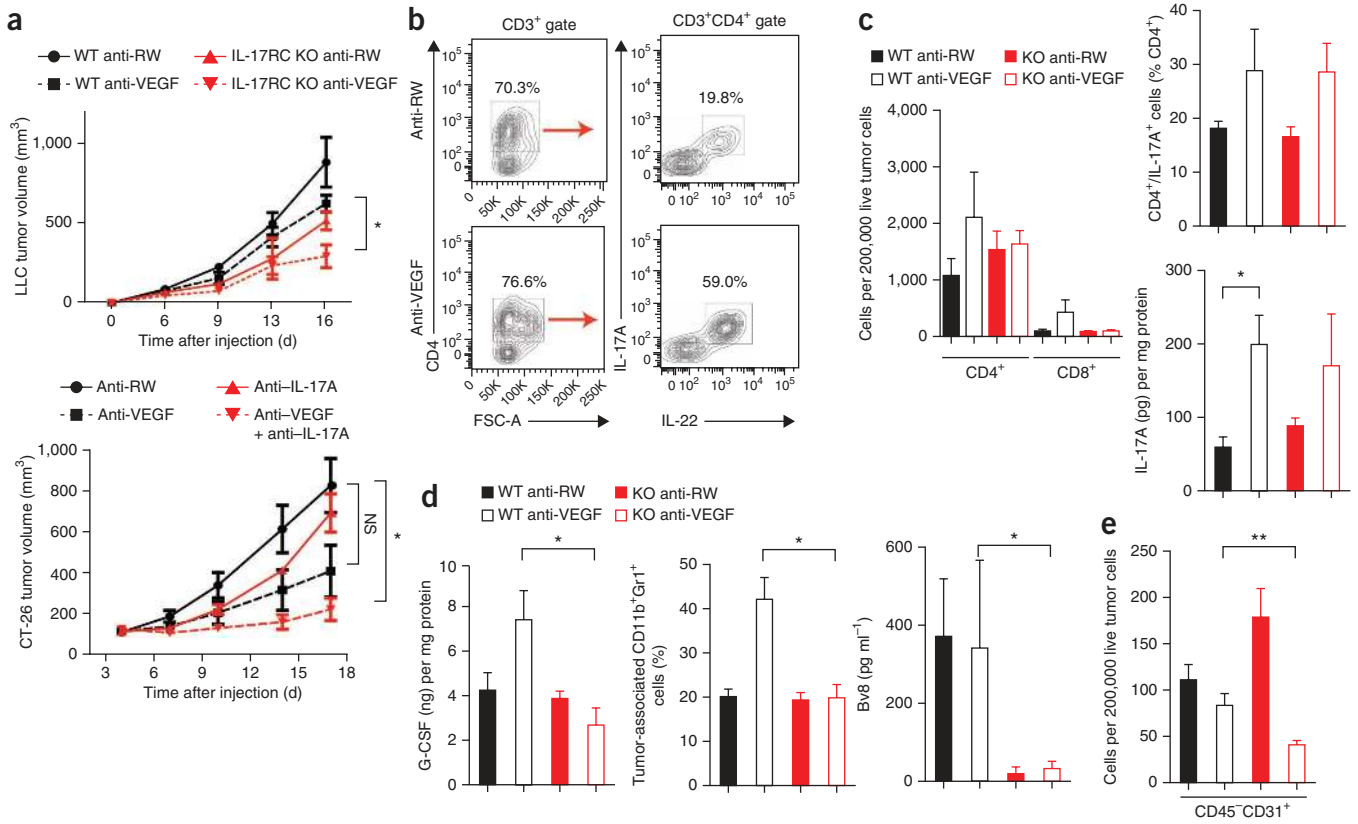

Figure 6 T_H17 cells mediate resistance to treatment with antibodies to VEGF through the recruitment to and activation of $CD11b^+Gr1^+$ cells in the tumor microenvironment. (**a**) Top, growth curves of syngeneic subcutaneous LLC tumors in WT and *Il17rc*$^{-/-}$ mice after administration of control antibodies (antibodies to ragweed) or antibodies to VEGF. Bottom, growth curves of syngeneic CT-26 tumors after administration of control antibodies, a neutralizing antibody to IL-17A, antibodies to VEGF or antibodies to IL-17A and VEGF in combination. $n = 8$ mice for each treatment group. (**b**) Percentages of $CD4^+$ and $CD4^+IL\text{-}17A^+IL\text{-}22^+$ TILs (gated in the boxes) isolated from LLC tumors in WT and *Il17rc*$^{-/-}$ mice treated with antibodies to VEGF or control antibodies, as assessed by flow cytometry. (**c**) Left, number of $CD4^+$ and $CD8^+$ TILs recovered in the indicated groups of mice. Top right, the percentage of $CD4^+IL\text{-}17^+IL\text{-}22^+$ cells out of the $CD4^+$ population quantified by flow cytometry. Bottom right, amounts of IL-17A, as assessed by ELISA, in tumors from WT and knockout hosts after administration of antibodies to ragweed or VEGF ($n = 5$–8 per group). (**d**) Quantification in LLC tumors in the indicated groups of mice of the amounts of G-CSF as measured by ELISA (left), the numbers of tumor-infiltrating $CD11b^+Gr1^+$ cells (middle) and the amounts of Bv8 (right) ($n = 5$–8 per group). (**e**) The numbers of tumor-associated endothelial cells in LLC tumor–bearing WT and knockout hosts as quantified by flow cytometry. $n = 5$–8 mice per group. All data are shown as the mean ± s.e.m. $^*P < 0.05$, $^{**}P < 0.005$ by two-tailed Student's *t* test. NS, not significant.

increased the numbers of both tumor-infiltrating $CD4^+$ and $CD8^+$ cells in WT hosts, although there were tenfold higher numbers of $CD4^+$ T cells compared to $CD8^+$ T cells (**Fig. 6b**,**c**). Although both of these mature T cell subpopulations are known to express IL-17, IL-17 expression was restricted to $CD4^+$ cells in the LLC tumors (**Fig. 6b**,**c** and **Supplementary Fig. 6a**). All $IL\text{-}17^+CD4^+$ cells in LLC tumors also expressed IL-22 (**Fig. 6b**), a hallmark cytokine for mature and terminally differentiated T_H17 cells[35]. We observed an increase in the $IL\text{-}17^+IL\text{-}22^+CD4^+$ population in LLC tumors in both WT and knockout hosts (**Fig. 6c**) after treatment with antibodies to VEGF. The increased prevalence of these tumor-infiltrating lymphocytes (TILs) in WT hosts treated with antibodies to VEGF coincided with increased amounts of both IL-17 and G-CSF in the tumor microenvironment, as well as with increased recruitment of $CD11b^+Gr1^+$ myeloid cells (**Fig. 6d**). Reduced recruitment of $CD11b^+Gr1^+$ cells in knockout compared to WT hosts in response to treatment with antibodies to VEGF corresponded to significant increases in $CD4^+$ and $CD8^+$ cell activation ($P < 0.05$), as well as to increases in the number of tumor-infiltrating T_H1 and interferon-γ (IFN-γ)$^+CD8^+$ T cells ($P < 0.05$) (**Supplementary Fig. 6b–d**). Together these data suggest an additional role for IL-17 in the suppression of antitumor T cell activity after treatment with antibodies to VEGF, probably through the recruitment of immune-suppressive $CD11b^+Gr1^+$ cells. Furthermore, the numbers of TAMs, including those defined as proangiogenic ($MRC1^{hi}CD11c^-$) or angiostatic ($MRC1^{lo}CD11c^+$)[24], were not significantly affected by IL-17 signaling within the tumor microenvironment (**Supplementary Fig. 6e**), indicating that these myeloid cell populations may not be a major contributor to the phenotype of refractoriness to VEGF-specific antibody treatment.

Recent studies have suggested that IL-17 has a role in promoting tumor angiogenesis[36,37], although most of these studies were performed with recombinant IL-17 protein or retroviral transduction of the IL-17 gene into tumors. We therefore studied the effect of endogenous tumor-infiltrating T_H17 cells on the tumor vasculature in our syngeneic LLC tumor model, comparing *Il17rc* knockout to WT hosts. We found that the presence of the angiogenic factor Bv8 within tumors depended on IL-17 signaling and that VEGF-specific antibody–mediated depletion of tumor-associated endothelial cells was enhanced in knockout hosts (**Fig. 6d**,**e**), indicating that endogenous T_H17 cells can promote persistent angiogenesis in the face of VEGF blockade. Pharmacological inhibition of IL-17 and Bv8 in combination produced no added effect compared to inhibition of either alone (**Supplementary Fig. 7**),

© 2013 Nature America, Inc. All rights reserved.

suggesting that these two molecules act in a linear pathway *in vivo*. In summary, our data provide evidence for the requirement of tumor-infiltrating T_H17 cells and IL-17 signaling within the host microenvironment in promoting expression of G-CSF and recruitment of immune-suppressive and proangiogenic $CD11b^+Gr^+$ cells, thereby mediating resistance to VEGF-specific antibody therapy.

DISCUSSION

Here we demonstrate that tumor-infiltrating T_H17 cells and an intact IL-17 signaling pathway in the tumor microenvironment are responsible for mediating resistance to the anti-angiogenic and antitumor effects of VEGF blockade across several tumor types. IL-17 has a role in promoting a proinflammatory tumor microenvironment by inducing cytokine expression from TAFs, most notably G-CSF. G-CSF is crucial for the mobilization and recruitment of $CD11b^+Gr1^+$ myeloid cells to the tumor microenvironment that are capable of promoting VEGF-independent tumorigenesis. In addition, IL-17 enhances the proangiogenic function of these bone marrow–derived cells through expression of VEGF and Bv8, as expression of these two factors is attenuated in *Il17rc*$^{-/-}$ tumor-bearing mice. We further demonstrate a strong correlation between tumor infiltration of Bv8-expressing polymorphonuclear granulocytes and T_H17 cells in human colorectal cancer, both of which are features of poor clinical outcome, indicating the relevance of our findings to human disease. Taken together, these findings demonstrate the role of adaptive immunity in mediating resistance to VEGF-specific antibody therapy.

Previous studies investigating tumor resistance to anti-angiogenic therapies have identified potential resistance mechanisms, including the recruitment of myeloid-derived suppressor cells and a role for tumor-associated fibroblasts in the expression of resistance-promoting factors (reviewed in ref. 38). This previous work raised the question of how interactions between the tumor and the normal host stroma promote resistance to VEGF blockade, leading us to uncover a crucial role for T_H17 cells and their canonical cytokine, IL-17, in mediating this process by eliciting G-CSF–dependent inflammation. Indeed, the tumor-suppressive effects of VEGF-specific antibodies in IL-17RC–deficient mice were largely recapitulated in G-CSFR–deficient mice, underscoring the importance of the IL-17–G-CSF signaling axis in resistance to VEGF blockade. Notably, we found that providing IL-17 to the tumor milieu was sufficient to produce resistance in a sensitive tumor type (Tib-6) in *nu*/*nu* mice, indicating that the effects of IL-17 on drug resistance do not require assistance from other T cell subsets such as T_H1 or cytotoxic T cells.

Abnormal myelopoiesis and tumor recruitment of immature myeloid cells is a common feature of tumor progression, although additional factors within the tumor microenvironment may be necessary for activating the immunosuppressive function of $CD11b^+Gr1^+$ MDSCs[21]. Our data show greatly impaired expression of tumor- and vasculature-promoting factors in $IL\text{-}17RC^-$ MDSCs compared to $IL\text{-}17RC^+$ MDSCs. Therefore, in addition to affecting the recruitment of immature myeloid cells to the tumor site, our data also indicate an additional role for T_H17 cells recruited to the tumor microenvironment in facilitating the activation of MDSCs and their function in establishing a VEGF-independent proangiogenic milieu.

Our findings are consistent with previous reports that IL-17 is required for tumor promotion in preclinical models[8], including a study that reported the ability of IL-17 to recruit MDSCs, such as $CD11b^+Gr1^+$ cells, to the tumor environment to promote tumor growth[39]. Although we did not observe this phenomenon in all tumor models tested, our study demonstrates the importance for IL-17 signaling not only in cell recruitment but also for the function of tumor stroma. Together our findings reinforce the importance of the IL-17–G-CSF–Bv8 axis in mediating VEGF-independent tumor angiogenesis *in vivo*, although we do not rule out a possible direct proangiogenic contribution of IL-17 (**Supplementary Fig. 8**).

That the resistance of the tumor models used in this study, the EL4 and LLC cell lines, to VEGF blockade is fully independent of VEGF function is also supported by recent findings documenting the resistance of these cell lines to sunitinib and axitinib, two potent US Food and Drug Association–approved small-molecule inhibitors that target the tyrosine kinase activity of VEGF receptors[40]. This class of molecules has been shown to inhibit both paracrine and intracrine VEGF signaling[41,42]. Thus, intracellular VEGF signaling, which is not blocked by antibodies, is probably not a contributing factor to the refractory phenotype of these tumor models.

Our data parallels recent findings revealing that IL-9 expressed by IL-17–deficient ROR-γ^-CD4^+ T cells mediates tumor suppression in tumor models similar to those used in our study[43]. In contrast, T_H17 cells have also been associated with tumor suppression and better prognosis in both preclinical models and patient populations[10]. Proposed explanations for these discrepancies broadly suggest a pro-tumor IL-17 effect in immunodeficient mice compared to an antitumor effect in immunocompetent mice[8]. Our findings, however, are inconsistent with an antitumor effect of T_H17 cells in immunocompetent mice, as we documented IL-17–dependent tumor growth and resistance to VEGF blockade in syngeneic tumor models. It is also unlikely that IL-22, a T_H17 cell–derived cytokine, influences stromal function, as IL-22 receptor expression is limited to epithelial cells of the digestive organs, respiratory tract and skin[44]. Our findings in preclinical models of lung and colorectal cancer are consistent with clinical reports that the presence of T_H17 immune infiltrates correlates with worse prognosis and overall survival, whereas their presence correlates with better outcomes in other tumor types, such as ovarian and gastric cancers[10]. These divergent clinical findings highlight the effect of the tumor context in informing the function of immune infiltrates and argue that care is needed in selecting tumor types that might be treated with IL-17-specific antibodies.

Crosstalk between adaptive and innate immunity in mediating tumor resistance to VEGF blockade has not been previously reported. Our studies show that inhibiting T_H17 cells and their paracrine function in the tumor microenvironment substantially enhances the tumor response to VEGF blockade. Further studies will be needed to determine how generalizable these findings are to additional tumor types and whether tumor-infiltrating immune cells could serve as biomarkers for stratifying patients for their responsiveness to VEGF blockade, such as with bevacizumab. It also remains to be established whether IL-17 mediates resistance to targeted therapies other than anti-angiogenic agents. Our findings have the potential to improve the clinical efficacy of VEGF-targeting agents through inhibition of T_H17 cell function.

METHODS

Methods and any associated references are available in the online version of the paper.

Note: Any Supplementary Information and Source Data files are available in the online version of the paper.

ACKNOWLEDGMENTS

We thank R. Khosla, I. Mellman, J. Kim, V. Phan, M. Yan and M. Junttila for helpful discussions and comments. We thank L. Komuves, C. Chalouni, M. Gonzales Edick

© 2013 Nature America, Inc. All rights reserved.

and M. Sagolla for providing microscopy expertise and Genentech microarrays (in particular, Z. Modrusan), the Genentech animal and FACS facilities (in particular, A. Paler-Martinez) and D. Kallop and R. Weimer in animal imaging at Genentech. We thank N. Ota for help with *Il17rc*$^{-/-}$ mice.

AUTHOR CONTRIBUTIONS

A.S.C. designed, planned and coordinated the experiments, analyzed the data and wrote the manuscript. N.F. coordinated and supervised the project and wrote the manuscript. A.S.C., X.W. and G.Z. performed the experiments. W.O. provided study design. Z.J. performed microarrays and bioinformatics analysis. H.N. and I.K. assisted with image acquisition and performed the analyses of clinical and preclinical samples, respectively. F.V.P. provided pathologist review and assessment of clinical samples. J.Z. and Y.G.M. performed mouse Bv8 ELISA. J.-M.V. and Y.G.M. performed intratumoral antibody ELISAs.

COMPETING FINANCIAL INTERESTS

The authors declare competing financial interests: details are available in the online version of the paper.

Reprints and permissions information is available online at http://www.nature.com/reprints/index.html.

1. Ferrara, N. & Kerbel, R.S. Angiogenesis as a therapeutic target. *Nature* **438**, 967–974 (2005).
2. Bergers, G. & Hanahan, D. Modes of resistance to anti-angiogenic therapy. *Nat. Rev. Cancer* **8**, 592–603 (2008).
3. Ellis, L.M. & Hicklin, D.J. VEGF-targeted therapy: mechanisms of anti-tumour activity. *Nat. Rev. Cancer* **8**, 579–591 (2008).
4. Tlsty, T.D. & Coussens, L.M. Tumor stroma and regulation of cancer development. *Annu. Rev. Pathol.* **1**, 119–150 (2006).
5. Ebos, J.M., Lee, C.R. & Kerbel, R.S. Tumor and host-mediated pathways of resistance and disease progression in response to antiangiogenic therapy. *Clin. Cancer Res.* **15**, 5020–5025 (2009).
6. Hanahan, D. & Coussens, L.M. Accessories to the crime: functions of cells recruited to the tumor microenvironment. *Cancer Cell* **21**, 309–322 (2012).
7. Crawford, Y. & Ferrara, N. VEGF inhibition: insights from preclinical and clinical studies. *Cell Tissue Res.* **335**, 261–269 (2009).
8. Maniati, E., Soper, R. & Hagemann, T. Up for mischief? IL-17/Th17 in the tumour microenvironment. *Oncogene* **29**, 5653–5662 (2010).
9. Grivennikov, S.I. *et al.* Adenoma-linked barrier defects and microbial products drive IL-23/IL-17–mediated tumour growth. *Nature* **491**, 254–258 (2012).
10. Fridman, W.H., Pages, F., Sautes-Fridman, C. & Galon, J. The immune contexture in human tumours: impact on clinical outcome. *Nat. Rev. Cancer* **12**, 298–306 (2012).
11. Shojaei, F. *et al.* Tumor refractoriness to anti-VEGF treatment is mediated by CD11b+Gr1+ myeloid cells. *Nat. Biotechnol.* **25**, 911–920 (2007).
12. Crawford, Y. *et al.* PDGF-C mediates the angiogenic and tumorigenic properties of fibroblasts associated with tumors refractory to anti-VEGF treatment. *Cancer Cell* **15**, 21–34 (2009).
13. Shojaei, F. *et al.* G-CSF–initiated myeloid cell mobilization and angiogenesis mediate tumor refractoriness to anti-VEGF therapy in mouse models. *Proc. Natl. Acad. Sci. USA* **106**, 6742–6747 (2009).
14. Iwakura, Y., Ishigame, H., Saijo, S. & Nakae, S. Functional specialization of interleukin-17 family members. *Immunity* **34**, 149–162 (2011).
15. Korn, T., Bettelli, E., Oukka, M. & Kuchroo, V.K. IL-17 and Th17 Cells. *Annu. Rev. Immunol.* **27**, 485–517 (2009).
16. Qu, X., Zhuang, G., Yu, L., Meng, G. & Ferrara, N. Induction of Bv8 expression by granulocyte colony-stimulating factor in CD11b+Gr1+ cells: key role of Stat3 signaling. *J. Biol. Chem.* **287**, 19574–19584 (2012).
17. Shojaei, F. *et al.* Bv8 regulates myeloid-cell–dependent tumour angiogenesis. *Nature* **450**, 825–831 (2007).
18. Hu, Y. *et al.* IL-17RC is required for IL-17A– and IL-17F–dependent signaling and the pathogenesis of experimental autoimmune encephalomyelitis. *J. Immunol.* **184**, 4307–4316 (2010).
19. Metcalf, D. The molecular control of cell division, differentiation commitment and maturation in haemopoietic cells. *Nature* **339**, 27–30 (1989).
20. Gabrilovich, D.I. & Nagaraj, S. Myeloid-derived suppressor cells as regulators of the immune system. *Nat. Rev. Immunol.* **9**, 162–174 (2009).
21. Gabrilovich, D.I., Ostrand-Rosenberg, S. & Bronte, V. Coordinated regulation of myeloid cells by tumours. *Nat. Rev. Immunol.* **12**, 253–268 (2012).
22. Shojaei, F. & Ferrara, N. Refractoriness to antivascular endothelial growth factor treatment: role of myeloid cells. *Cancer Res.* **68**, 5501–5504 (2008).
23. Sinha, P. *et al.* Proinflammatory S100 proteins regulate the accumulation of myeloid-derived suppressor cells. *J. Immunol.* **181**, 4666–4675 (2008).
24. Mazzieri, R. *et al.* Targeting the ANG2/TIE2 axis inhibits tumor growth and metastasis by impairing angiogenesis and disabling rebounds of proangiogenic myeloid cells. *Cancer Cell* **19**, 512–526 (2011).
25. Erez, N., Truitt, M., Olson, P., Arron, S.T. & Hanahan, D. Cancer-associated fibroblasts are activated in incipient neoplasia to orchestrate tumor-promoting inflammation in an NF-κB–dependent manner. *Cancer Cell* **17**, 135–147 (2010).
26. Bettelli, E., Korn, T., Oukka, M. & Kuchroo, V.K. Induction and effector functions of T_H17 cells. *Nature* **453**, 1051–1057 (2008).
27. Weaver, C.T., Hatton, R.D., Mangan, P.R. & Harrington, L.E. IL-17 family cytokines and the expanding diversity of effector T cell lineages. *Annu. Rev. Immunol.* **25**, 821–852 (2007).
28. Dong, C. Diversification of T-helper-cell lineages: finding the family root of IL-17–producing cells. *Nat. Rev. Immunol.* **6**, 329–333 (2006).
29. Tosolini, M. *et al.* Clinical impact of different classes of infiltrating T cytotoxic and helper cells (Th1, Th2, Treg, Th17) in patients with colorectal cancer. *Cancer Res.* **71**, 1263–1271 (2011).
30. Liu, J. *et al.* IL-17 is associated with poor prognosis and promotes angiogenesis via stimulating VEGF production of cancer cells in colorectal carcinoma. *Biochem. Biophys. Res. Commun.* **407**, 348–354 (2011).
31. Chen, X. *et al.* Increased IL-17–producing cells correlate with poor survival and lymphangiogenesis in NSCLC patients. *Lung Cancer* **69**, 348–354 (2010).
32. Dirkx, A.E. *et al.* Anti-angiogenesis therapy can overcome endothelial cell anergy and promote leukocyte-endothelium interactions and infiltration in tumors. *FASEB J.* **20**, 621–630 (2006).
33. Shrimali, R.K. *et al.* Antiangiogenic agents can increase lymphocyte infiltration into tumor and enhance the effectiveness of adoptive immunotherapy of cancer. *Cancer Res.* **70**, 6171–6180 (2010).
34. Manning, E.A. *et al.* A vascular endothelial growth factor receptor-2 inhibitor enhances antitumor immunity through an immune-based mechanism. *Clin. Cancer Res.* **13**, 3951–3959 (2007).
35. McGeachy, M.J. *et al.* TGF-β and IL-6 drive the production of IL-17 and IL-10 by T cells and restrain T_H-17 cell-mediated pathology. *Nat. Immunol.* **8**, 1390–1397 (2007).
36. Tartour, E. *et al.* Interleukin 17, a T-cell–derived cytokine, promotes tumorigenicity of human cervical tumors in nude mice. *Cancer Res.* **59**, 3698–3704 (1999).
37. Numasaki, M. *et al.* Interleukin-17 promotes angiogenesis and tumor growth. *Blood* **101**, 2620–2627 (2003).
38. Chung, A.S., Lee, J. & Ferrara, N. Targeting the tumour vasculature: insights from physiological angiogenesis. *Nat. Rev. Cancer* **10**, 505–514 (2010).
39. He, D. *et al.* IL-17 promotes tumor development through the induction of tumor promoting microenvironments at tumor sites and myeloid-derived suppressor cells. *J. Immunol.* **184**, 2281–2288 (2010).
40. Shojaei, F. *et al.* HGF/c-Met acts as an alternative angiogenic pathway in sunitinib-resistant tumors. *Cancer Res.* **70**, 10090–10100 (2010).
41. Gerber, H.P. *et al.* VEGF regulates haematopoietic stem cell survival by an internal autocrine loop mechanism. *Nature* **417**, 954–958 (2002).
42. Lee, S. *et al.* Autocrine VEGF signaling is required for vascular homeostasis. *Cell* **130**, 691–703 (2007).
43. Purwar, R. *et al.* Robust tumor immunity to melanoma mediated by interleukin-9–producing T cells. *Nat. Med.* **18**, 1248–1253 (2012).
44. Curd, L.M., Favors, S.E. & Gregg, R.K. Pro-tumour activity of interleukin-22 in HPAFII human pancreatic cancer cells. *Clin. Exp. Immunol.* **168**, 192–199 (2012).

© 2013 Nature America, Inc. All rights reserved.

ONLINE METHODS

Cell lines. Mouse tumor cell lines (EL4, Tib-6, LLC and CT-26) were obtained from the American Type Culture Collection (ATCC). The cell lines were cultured in DMEM or RPMI (for CT-26) (Invitrogen, Carlsbad, CA). Media were supplemented with L-glutamine and 10% FBS (Sigma, St. Louis, MO). All cells were cultured and maintained at 37 °C in a 5% CO_2 and 80% humidity incubator and were free of mycoplasma contamination. Primary mouse fibroblasts from WT and knockout mice were obtained from laboratory of W.O.[18] and recovered in DMEM for up to 48 h prior to the indicated assays. Tib-6 cells were stably transfected with either pRK-neo or pRK–neo–IL-17A plasmids and selected with neomycin followed by single-cell cloning. Mouse cDNA expressing full-length IL-17A (GenBank accession U35108.1) was generated by PCR and cloned into a pRK-5 vector (BD Biosciences). Two stable Tib-6–neo control and four Tib-6–IL-17A clones were subsequently analyzed *in vivo*.

RNA sample preparation and qRT-PCR analysis. Total DNA-free RNA was isolated with the RNeasy kit (Qiagen, Germany) according to the manufacturer's protocol. One-step qRT-PCR was done in a total volume of 50 µl with the SuperScript III Platinum One-Step qRT-PCR Kit (Invitrogen, Carlsbad, CA) or with TaqMan One-Step RT-PCR Master Mix (Applied Biosystems, Foster City, CA). The following TaqMan Gene Expression Assay primers and probe mixes were used for the following mouse genes: *Il17* (Mm00439619_m1), *Il6* (Mm01210733_m1), *Bv8* (also known as *Prok2*; Mm00450080_m1), *G-CSF* (also known as *Csf3*; Mm00438334_m1), *Mmp9* (Mm00442991_m1), *S100a8* (Mm00496696_g1), *S100a9* (Mm00656925_m1) and *Gapdh* (Mm99999915_g1). Analyses were carried out on a standard ABI 7500 machine (Invitrogen) according to the manufacturer's recommended protocols.

Microarray analysis. Single-cell suspensions were prepared from tumors isolated from tumor-bearing mice, and the $CD11b^+Gr1^+$ and $CD11b^+Gr1^-$ populations were labeled with antibodies to CD11b (M1/70, eBiosciences) and Gr1 (RB6-8C5, eBiosciences) and purified by FACS of live cells. Both antibodies were used at 1:100 dilution. Total RNA was isolated using the Qiagen RNAeasy Kit following the manufacturer's instructions. RNA quality was verified by running samples on an Agilent Bioanalyzer 2100. Samples were labeled by two rounds of amplification using the Ambion MessageAmpII aRNA Amplification Kit and the Agilent QuickAmp Labeling Kit. For all samples, 750 ng of labeled cRNA was fragmented and hybridized against the Cy3-labeled universal mouse reference (Stratagene, La Jolla, CA). The Agilent *In situ* Hybridization Kit Plus was used when Cy dye–differentially labeled control and test samples were applied to microarrays enclosed in Agilent SureHyb-enabled hybridization chambers. After hybridization, the arrays were washed twice, dried and then scanned on an Agilent scanner, and images were processed using Agilent Feature Extraction software version 10.7. Agilent Feature Extraction software version 10.7 was used to create feature extraction files. The normal exponential convolution model was applied for background correction. Loess normalization done within an array (that is, for all of the spots), and quantile normalization was done across all of the arrays that are part of an experiment. Gene differential expression was analyzed using the Limma package. The normalized log2 ratio (Cy5/Cy3) was used to represent the test-to-reference ratio. Microarray data are deposited in the NCBI Gene Expression Omnibus (GEO) under accession code GSE48329.

Collection of conditioned medium from tumor cells. EL4 and Tib-6 cell lines were grown in six-well plates at a density of 1×10^6 ml^{-1} in low-serum DMEM (1% FBS) for 72 h. Cell viability and total cell numbers were measured using a Vi-Cell XR Cell Analyzer instrument (Beckman Coulter, Fullerton, CA) to account for changes in cell numbers during the conditioning period. All data were normalized by cell number at the end of the conditioning period. All experimental conditions included three biological replicates, and all experiments were independently repeated at least twice.

Cytokine bead assays and ELISA. Sera and supernatants from isolated cells collected after 72 h of culture were analyzed with the Bio-Plex Pro Magnetic Cytokine, Chemokine and Growth Factor Assays system (BioRad, Hercules, CA). Cells were cultured in reduced-serum medium (1% FBS). The amounts of mouse IL-17A, G-CSF and IL-6 were measured by a Quantikine ELISA kit (R&D Systems, Minneapolis, MN). Bv8 concentrations were measured by ELISA as described previously[13]. All experiments consisted of at least five biological replicates per condition and were independently performed at least three times.

Mice. Female and male mice (6–12 weeks old) were used as follows: $Il17rc^{-/-}$ and WT littermates both in a C57BL/6 genetic background (ref. 18) were bred and maintained at Genentech, Inc. under specific pathogen-free conditions. Female WT C57BL/6 and *nu*/*nu* mice were purchased from Charles River Laboratory (Hollister, CA). Procedures involving animals were reviewed and approved by the Institutional Animal Care and Use Committee (IACUC) at Genentech, Inc. and conformed to regulatory and ethical standards. Study sample sizes were based on historical efficacy data for the agents used in this manuscript. The studies were powered to achieve statistical significance. Mouse groupings and randomization were performed in studies using luciferase-positive LLCs to ensure a balanced distribution of tumor volumes across all groups of the study. The mouse studies were not blinded, as the same investigators performed the grouping, dosing and analyses, rendering blinding of the studies unfeasible.

Tumor models and antibodies. *Subcutaneous models.* EL4, LLC, CT-26, Tib-6–neo and Tib-6–IL-17 tumor cells (2.0×10^6) in 100 µl of growth factor–reduced Matrigel (BD BioScience) were subcutaneously inoculated in the dorsal flank of mice of the indicated genotypes as shown in the figures.

Orthotopic model. Six- to eight-week-old C57BL/6 WT mice were anesthetized with isoflurane and placed in the right lateral decubitus position. A 5-mm skin incision overlying the left chest wall was made, and the left lung was visualized through the pleura. A total of 5.0×10^5 LLC-luciferase cells (Caliper LifeSciences, Hopkinton, MA) (single-cell suspensions, >90% viability) in 10 µl of a solution of growth factor–reduced Matrigel (BD Biosciences) and PBS were injected into the left lungs of the mice through the pleura with a 30-gauge needle. After tumor cell injection, the wound was stapled, and the mice were placed in the left lateral decubitus position and observed until they fully recovered.

Antibodies were intraperitoneally injected twice per week at 10 mg per kg body weight unless otherwise noted. Treatments with control antibody to ragweed (generated at Genentech), the monoclonal antibody B20-4.1.1 to VEGF or antibodies to IL-17A, IL-17F or IL-17A/F were initiated 2 d after tumor cell inoculation. The moncolonal antibody B20-4.1.1 neutralizes the activity of all isoforms and proteolytic fragments of VEGF-A[45]. Monoclonal antibodies specific for mouse IL-17A, IL-17F and IL-17A/F were generated at Genentech. The monoclonal antibodies 2B9 and 3F1 to human (crossreactive with mouse) Bv8 were administered together as previously described[17]. All tumor growth experiments were performed in three independent studies and conducted in accordance with the Genentech Guide for the Care and Use of Laboratory Animals. Mice that lost >20% body weight or with ulcerated tumors were excluded from the study, and their condition was discussed with the veterinary staff. Additionally, mice observed to have unexpected adverse effects were visually monitored twice a week, with increased frequency of monitoring up to daily depending on the severity of their condition. Tumor volumes were calculated using the ellipsoid volume formula ($0.5 \times l \times w^2$, where l is length and w is width).

Patient samples. Human surgical material was obtained after receiving informed consent using a Genentech Institutional Review Board–approved protocol. Paraffin-embedded tissues containing primary colorectal cancer samples were obtained from the Genentech Pathology Core Tissue Bank in compliance with protocols approved by the Genentech Institutional Review Board.

Flow cytometry. Mononuclear cells were isolated from bone marrow extracted from mouse femurs and from peripheral blood through cardiac puncture, and tumor cells were harvested from mice implanted with tumors. Tumors from mice treated with control antibodies and mice treated with antibodies to VEGF were isolated, and single-cell suspensions were obtained by mincing tumors with razor blades and homogenizing them by mechanical disruption and digestion with Collagenase/Dispase and DNase (Roche, Basel, Switzerland) at 1 mg ml^{-1} in growth medium for 1 h at 37 °C. Red blood cells were lysed using ACK lysis buffer (Lonza, Basel, Switzerland), followed by staining with rat antibodies to mouse CD11b (M1/70), Gr1 (RB6-8C5) and Ly6G (BD Bioscience, San Jose, CA).

© 2013 Nature America, Inc. All rights reserved.

For T cell analysis, antibodies to the following mouse proteins from eBiosciences were used: CD3 (145-2C11), IL-17A (eBio17B7), IL-22 (1H8PWSR), forkhead box P3 (FOXP3) (FJK-16s) and CD44 (IM7). Antibodies to the following mouse proteins from R&D Systems were also used: CD4 (GK1.5), CD8 (53-6.) and IFN-γ (37895). The dilution for all antibodies was 1:100 with the exception of Gr-1 (1:200). Intracellular cytokine staining was performed according to the manufacturer's protocols. To exclude dead cells, propidium iodide (Sigma, St. Louis, MO) was added to all samples before data acquisition on an LSRIIB FACS instrument (BD Biosciences) and analysis using FlowJo software (Tree Star, Ashland, OR).

Isolation of $CD11b^+Gr1^+$ cells from spleen and functional T cell suppression assay. Single-cell suspensions were prepared from spleens isolated from tumor-naive and tumor-bearing mice by mincing spleens with razor blades and homogenizing them by mechanical disruption and digestion with Collagenase/Dispase and DNase (Roche, Basel, Switzerland) at 1 mg ml^{-1} in growth medium for 1 h at 37 °C. The $CD11b^+Gr1^+$ population was sorted by labeling cells first with a monoclonal antibody to Gr1-phycoerythrin (PE) conjugate (RB6-8C5) and then with anti-PE biotinylated microbeads (for magnetic-activated cell sorting (MACS); Miltenyi Biotech, Bergisch-Gladbach, Germany) according to protocols provided by the manufacturer. An aliquot of the $Gr1^+$ sorted cells was stained with antibodies to CD11b and Gr1 and analyzed by FACS to ensure the purity (>90%) of the $CD11b^+Gr1^+$ cells.

Polyclonal suppression of T cells was evaluated in a coculture assay in which T cells isolated from splenocytes from either tumor-bearing mice or naive mice (polyclonal assay) were seeded in triplicates in 96-well flat bottom plates (3×10^5 per well). T cells were isolated using negative selection with the Pan-T cell isolation kit (Miltenyi Biotech). T cells were cultured in the presence of tumor-associated $Gr1^+CD11b^+$ cells and either left untreated or stimulated with antibodies to CD3 (0.5 mg ml^{-1}, BD Biosciences, 145-2C11) and CD28 (1 mg ml^{-1}, BD Biosciences, 37.51). On day 3 of the coculture, cells were labeled with CFSE (Invitrogen). T cells were evaluated on day 3 by flow cytometry for CFSE dilution.

CFSE labeling of mouse cells. Cells were resuspended at $10–20 \times 10^6$ cells per ml in a minimum volume of 500 ml PBS and incubated with CFSE (0.5 mM) at room temperature for 8 min with constant swirling. The reaction was then quenched with medium containing 10% FBS.

Immunohistochemistry. Tumor samples were embedded in Optimum Cutting Temperature compound (OCT; Sakura Finetek) and frozen in a dry-ice bath. Tumor sections were cut (10 μm) in a cryostat (Leica Microsystem). Sections were dried at 20 °C for 1 h and then fixed in acetone for 10 min at −20 °C. After air drying, nonspecific binding sites were blocked by incubation for 1 h at 20 °C in 10% normal donkey serum (Jackson ImmunoResearch, West Grove, PA) followed by immunostaining with antibodies diluted in 1.5% normal serum in 2% BSA and PBS. Tumor sections were stained with the following primary antibodies: rat antibodies to mouse CD31 (MEC13.3, BD Pharmingen) at 1:100 overnight at 4 °C, antibodies to rabbit desmin (GTX15200, Genetex) at 1:400 and antibodies to mouse SMA-Cy3 conjugate (1A4, Sigma) overnight at 4 °C, followed by secondary antibodies, antibodies to rat Alexa-488 conjugate and antibodies to rabbit Alexa-647 conjugate (Invitrogen) for 2 h at 20 °C. The slides were counterstained with DAPI, washed and mounted in DAKO fluorescent mounting medium (DakoCytomation). Immunofluorescence images were collected on a Zeiss AxioImager Z2 upright microscope (Zeiss) and a TissueGnostics Slide scanner (TissueGnostics, Vienna, Austria).

Formalin-fixed paraffin-embedded tissues were sectioned (4 μm) for immunohistochemistry. After rehydration, sections were treated in DAKO Target Retrieval (DAKO) for 20 min in a water bath at 99 °C and cooled for 20 min for antigen retrieval. Sections were then blocked with 10% serum and 3% BSA and PBS for 1 h at room temperature and then incubated with rabbit antibodies to human IL-17A (AF-317-NA, R&D Systems) or the monoclonal antibody 3F1 to Bv8 (ref. 46) overnight at 4 °C. The secondary antibody used was biotinylated goat antibody to rabbit IgG (Vector Laboratories).

Image acquisition and analysis. Tumor mean vessel density was quantified from digital images captured on the TissueGnostics Slide scanner of CD31-stained sections using a ×20 objective. The pixels corresponding to stained vessels were selected using Definiens Tissue Studio Software (Definiens, New Jersey). Whole-tumor cross-sections and a total of five tumors per group were analyzed. The aggregate pixel vessel area, relative to the total picture area and total area analyzed, is reported as a percentage of the positive cellular area relative to the total surface area.

IL-17A-positive T_H17 cells and Bv8-positive cells were quantified within the perimeter of the tumor region that was manually identified and drawn on digital whole-slide images acquired using the Nanozoomer system (Hamamatsu, Bridgewater, NJ) and within the peripheral area surrounding the tumor as determined by a 500-μm perimeter area surrounding the tumor regions of interest. Positive Bv8 or T_H17 and hematoxylin staining were quantified using a blue-normalization algorithm[47].

Statistical analyses. Student's *t* test (two-tailed) was used to determine significant differences in all experiments. $P < 0.05$ was considered significant.

45. Liang, W.C. *et al.* Cross-species vascular endothelial growth factor (VEGF)-blocking antibodies completely inhibit the growth of human tumor xenografts and measure the contribution of stromal VEGF. *J. Biol. Chem.* **281**, 951–961 (2006).
46. Zhong, C., Qu, X., Tan, M., Meng, Y.G. & Ferrara, N. Characterization and regulation of Bv8 in human blood cells. *Clin. Cancer Res.* **15**, 2675–2684 (2009).
47. Brey, E.M. *et al.* Automated selection of DAB-labeled tissue for immunohistochemical quantification. *J. Histochem. Cytochem.* **51**, 575–584 (2003).

© 2013 Nature America, Inc. All rights reserved.

doi:10.1038/nm.3291